NASA
Technical Memorandum 101435

AVSCOM
Technical Report 88-C-032

The Role of Thermal and Lubricant Boundary Layers in the Transient Thermal Analysis of Spur Gears

L.E. El-Bayoumy and L.S. Akin
California State University
Long Beach, California

D.P. Townsend
Lewis Research Center
Cleveland, Ohio

and

F.C. Choy
University of Akron
Akron, Ohio

Prepared for the
Fifth International Power Transmission and Gearing Conference
sponsored by the American Society of Mechanical Engineers
Chicago, Illinois, April 25-27, 1989

NASA

US ARMY
AVIATION
SYSTEMS COMMAND
AVIATION R&T ACTIVITY

THE ROLE OF THERMAL AND LUBRICANT BOUNDARY LAYERS IN THE TRANSIENT THERMAL ANALYSIS OF SPUR GEARS

L.E. El-Bayoumy and L.S. Akin
California State University
Long Beach, California 90840

D.P. Townsend
National Aeronautics and Space Administration
Lewis Research Center
Cleveland, Ohio 44135

and

F.C. Choy
University of Akron
Akron, Ohio 44325

ABSTRACT

An improved convection heat-transfer model has been developed for the prediction of the transient tooth surface temperature of spur gears. The dissipative quality of the lubricating fluid is shown to be limited to the capacity extent of the thermal boundary layer. This phenomenon can be of significance in the determination of the thermal limit of gears accelerating to the point where gear scoring occurs. Steady-state temperature prediction is improved considerably through the use of a variable integration time step that substantially reduces computer time. Computer-generated plots of temperature contours enable the user to animate the propagation of the thermal wave as the gears come into and out of contact, thus contributing to better understanding of this complex problem. This model has a much better capability at predicting gear-tooth temperatures than previous models.

E-4413

NOMENCLATURE

A	heat flux area, m^2 ($in.^2$)
$\bar{a}$	acceleration of fluid particle, m/sec^2 ($in./sec^2$)
b	Herzian contact width, m (in.)
$\bar{C}$	heat capacitance matrix
C_a	dimensionless constant $(2R_o/F)^2$, see Eq. (9)
F	face width of tooth in contact, m (in.)
f	coefficient of friction
G	centrifugal acceleration, m/sec^2 ($in./sec^2$)
h_j	heat-transfer coefficient for lubricated flank of gear, W/hr m^2 K (Btu/hr ft^2 °F)
h_{jt}	heat-transfer coefficient for top land of gear, W/hr m^2 K (Btu/hr ft^2 °F)
h_s	heat-transfer coefficient for gear sides, W/hr m^2 K (Btu/hr ft^2 °F)
h_t	heat-transfer coefficient for unlubricated flank of gear, W/hr m^2 K (Btu/hr ft^2 °F)
J	heat-conversion factor
k	thermal conductivity, W/m K (Btu/ft °F)
N	number of teeth
n	normal coordinate to tooth profile, m (in.)
P_d	diameter to pitch ratio, m^{-1} ($in.^{-1}$)
q	heat flux, W/hr (Btu/hr)
R_o	addendum radius of gear, m (in.)
$\bar{r}$	radius vector of fluid particle, m (in.)
S	surface finish
s	tangential coordinate to the tooth profile, m (in.)
T	temperature, K (°F)
t	time, hr
V_s	instantaneous sliding velocity, m/sec (ft/sec)
V_t	instantaneous total velocity, m/sec (ft/sec)
W	normal tooth load intensity, N/m (lb/ft)
x,y,z	dimensionless Cartesian coordinates of gear tooth
α	thermal diffusivity, m^2/s ($in.^2/s$)
γ	finite difference weighting factor ($0 < \gamma < 1$)

θ dimensionless gear temperature

μ dynamic viscosity

ν kinematic viscosity

$\vec{\omega}$ angular velocity vector, sec^{-1}

INTRODUCTION

Recent trends in the design of high-speed machinery necessitated careful consideration of factors affecting gear durability. As a major failure mode of high-speed gearing, scoring is receiving significant attention. Scoring failures have been attributed to a sudden surge of the contact temperature of the gear. This contact temperature is directly related to the bulk temperature of the gear blank. Thus, an accurate prediction of scoring thresholds hinges on a correct evaluation of the bulk temperature. To evaluate the contact temperature, finite-element programs were developed by Patir (1977), Townsend (1981), and El-Bayoumy (1984) with the purpose of analyzing the steady-state thermal behavior of spur gears. The steady-state approximation required the assumption of constant heat-transfer coefficients. The numerical values of the coefficients were based on correlation with experimental measurements made by Townsend (1981). When operating conditions such as speed, applied load, initial temperature, and oil jet velocity, pressure, and viscosity were varied, correlation between theory and experiment was not always satisfactory.

The difficulties arising from having to assume the proper values for these heat-transfer coefficients were overcome in El-Bayoumy (1985), where a transient thermal analysis approach was developed. The convection process in El-Bayoumy (1985) was based on an extended model from Van Heijningen (1974) that yielded a set of time-dependent coefficients.

Closer examination of the hydrodynamic and thermal phenomena within the adjacent fluid film shows the film thickness remaining above the impingement point to decrease with time. The thermal boundary-layer thickness, on the other hand, grows steadily with time. An instant is therefore reached when the two thicknesses are equal. At that point the fluid film is fully saturated with heat and can no longer participate in the convection process. The wetted side of the gear tooth may therefore be divided into two regions: a convective region, where the heat-transfer coefficients, derived from the extended Blok model, can be used and a nonconvective region with vanishing heat-transfer coefficients.

The objective of this paper is to quantify the influence of the interaction between the thermal boundary and the oil film thickness on the transient thermal behavior of spur gears. In addition, the thermal wave propagation process of the hot spots are portrayed by instantaneous isotherms as they move through the gear tooth. The asymptotic approach towards steady state in the absence and presence of the thermal boundary layer is evaluated.

Interaction Between Thermal and Hydrodynamic Effects Within the Fluid Film

To evaluate how much of the adjacent lubricant actually contributes to the heat dissipation of the gear tooth, one needs to consider the hydrodynamic forces acting on a fluid particle near the tooth surface above and below the point of impingement.[1]

Considering a frame of reference, attached to the gear at its center of rotation and thus rotating with an angular velocity $\vec{\omega}$ (assumed constant), the acceleration of the fluid particle is given by

$$\vec{a} = -\vec{\omega} \times \vec{\omega} \times \vec{r} - 2\vec{\omega} \times \vec{V} \qquad (1)$$

where $\vec{r}$ is the radius vector to the particle, and $\vec{V}$ is the relative velocity of jet impingement. The two terms appearing on the right hand side of Eq. (1) are the centrifugal and coriolis acceleration components. Since $\vec{r}$ varies very little across the tooth, the centrifugal acceleration, for all practical purposes can be considered constant for points along the tooth profile. Its magnitude is V_g^2/r where V_g is the velocity of the gear, at the pitch point the centrifugal acceleration as seen from the sign in Eq. (1) tends to strip off the oil layer from the surface of the tooth. The magnitude of the second term, the coriolis acceleration, is $2V_gV_j/r$ where V_j is the magnitude of the jet velocity relative to the gear. Since V_j is of the same order of magnitude as V_g, the coriolis component cannot be neglected. For points on the tooth profile below impingement, the direction of the coriolis acceleration is normal to the tooth surface pointing outward. Conversely, for points above impingement the coriolis acceleration points inward, as illustrated in Fig. 1, establishing a "pseudo-gravitational" field. Thus, the initial area A of convection heat flux q, characterized by the equation

$$q = hA\,\Delta T \qquad (2)$$

covers the length of the tooth profile above the impingement point. How much of this area will participate in heat dissipation can be determined when the thermal and fluid boundary layers are examined versus time. The thicknesses of these layers as a function of time are schematically illustrated in Fig. 2. The viscous layer develops in a time of the same order of magnitude as the oil spread time which is negligible compared with the heat-transfer time. While the viscous forces tend to attach the oil film to the tooth surface, centrifugal acceleration tries to strip it off. The amount of film remaining on the surface has been determined by Jefferis (1967), who showed that the thickness of this oil film is given by

$$H_f = \sqrt{\frac{\nu x}{Gt}} \qquad (3)$$

where ν is the kinematic viscosity of the oil, x is the coordinate along the tooth profile measured from the impingement point (see Fig. 1), G is the centrifugal acceleration, and t is time. This relationship is depicted in Fig. 2 as a straight line with negative slope.

The thermal boundary layer thickness is growing as a function of time according to the deWinter and Bloc (1974) formula

$$H_t = 1.362\sqrt{\alpha t} \qquad (4)$$

where α is the thermal diffusivity of the oil. The distance x_1 from the point of impingement of the point at which the thermal boundary layer thicknesses of Eq. (3) is equal to the film thickness of Eq. (4) and is therefore given by

$$x_1 = 1.85\,\frac{G\alpha}{\nu}\,t^2 \qquad (5)$$

[1]The derivations given in this section are based on private communications with Dr. John Murdock of the Aerospace Corporation.

This is the point of heat saturation of the fluid film. For points on the tooth profile below this point (i.e., $x \leqq x_1$), the fluid no longer contributes to the convective dissipation of heat. In other words, point P_1 becomes the effective impingement point. For points above P_1, a heat-transfer coefficient based on the solution of the one-dimensional heat equation

$$\frac{\partial T}{\partial t} = \alpha \frac{\partial^2 T}{\partial y^2} \tag{6}$$

is used. This coefficient may be written as

$$h_j = K/(\pi \alpha t)^{1/2} \tag{7}$$

Mathematical Formulation of the Transient Thermal Problems in Gearing

As noted in El-Bayoumy (1985), the partial differential equation governing heat transfer within the gear sector shown in Figs. 3 and 4 is given by

$$\frac{\partial^2 \theta}{\partial x^2} + \frac{\partial^2 \theta}{\partial y^2} + C_a \frac{\partial^2 \theta}{\partial z^2} - \alpha R_o^2 \frac{\partial \theta}{\partial t} = 0 \tag{8}$$

where

$$\left.\begin{aligned} C_a &= \left(\frac{2R_o}{F}\right)^2 \\ x = \frac{X}{R_o}, \quad y &= \frac{Y}{R_o}, \quad z = \frac{Z}{F/2} \\ \theta &= \frac{kP_d(T - T_o)}{q_{av}} \end{aligned}\right\} \tag{9}$$

and where

T current gear temperature, °C (°F)

T_o initial gear temperature, °C (°F)

α gear diffusivity, m^2/s ($in.^2/s$)

k thermal conductivity of gear material, W/m K (Btu/ft °F)

R_o outside radius of gear, m (ft)

F face width of gear, m (ft)

q_{av} average generated heat flux through the gear profile, W/hr (Btu/hr)

The associated boundary conditions are

$$\left.\begin{aligned} \frac{\partial \theta}{\partial n} + \frac{h_j(s,t)R_o}{k}\theta - P_d R_o q^* = 0 \quad &\text{on} \quad \Gamma_j \\ \frac{\partial \theta}{\partial n} + \frac{h_t(s,t)R_o}{k}\theta = 0 \quad &\text{on} \quad \Gamma_t \\ \frac{\partial \theta}{\partial z} + \frac{h_s(t)F}{2k}\theta = 0 \quad &\text{on} \quad \Gamma_s \end{aligned}\right\} \tag{10}$$

where

$\bar{n}$ n/R_o

n normal coordinate to the tooth profile

h_j convective heat transfer coefficient in tooth profile above the effective point of impingement, W/hr-m^2 K (Btu/hr ft^2 °F)

h_s convective heat transfer coefficient on front and back of gear

h_{jt} convective heat transfer coefficient on top land

h_t convective heat transfer coefficient on remainder of tooth including bottom land

P_d dimentral pitch of gear, ($in.^{-1}$)

q^* q/q_{av}

Γ_j tooth involute boundary above saturation point

Γ_s front and back end faces of tooth

Γ_t remainder of tooth profile

It was possible in El-Bayoumy (1985) to reduce the above boundary value problem through discretization to the recurrence relation

$$(\bar{C}/\Delta t + \bar{H}\gamma)\bar{\theta}_{n+1} = [\bar{C}/\Delta t - \bar{H}(1 - 2)]\bar{\theta}_n + \bar{P} \tag{11}$$

where $\bar{C}$ and $\bar{H}$ are the capacitance and heat conductivity matrices, $\bar{\theta}_n$ is the dimensionless temperature vector at time t_n, and $0 < \gamma < 1$. As noted in Zienkiewicz (1977), for numerical stability $\gamma > 1/2$.

Frictional Heat Vector Options

The instantaneous heat generated during contact between the two gears may be written as

$$q = \frac{1}{Jb} Wf|V_s| \tag{12}$$

where

J mechanical equivalent of heat, W/Nm (Btu/ftlb)

W normal load intensity, N/m (lb/ft)

b width of contact region, m (ft)

f coefficient of friction

V_s instantaneous sliding velocity, m/s (ft/s)

Assuming an even split between the pinion and the gear, the frictional heat input to either gear is

$$q_1 = \frac{1}{2Jb} fWV_s \tag{13}$$

Various options from the literature (Anderson, 1981) are available for the calculation of the friction coefficient. The following choices are incorporated into the program (according to Kelly-Benedict, 1961):

$$f_1 = 0.0127 \log\left(\frac{3.17 \times 10^6 W}{F\mu V_S V_T^2}\right) \tag{14}$$

If the effect of surface finish is to be examined, a modified Kelly-Benedict formula is

$$f_2 = \left(\frac{S + 22}{35}\right) f_1 \qquad (15)$$

The results presented in this paper are based on the Kelley-Benedict formula (Eq. (14)) as it correlates well with efficiency measurements given in Anderson (1981).

RESULTS AND DISCUSSIONS

The heat-transfer coefficients derived in Eq. (7) were used in El-Bayoumy (1985) for all points above the true impingement point. The computer program developed for the purpose of evaluating transient thermal behavior was mainly concerned with numerical stability of two- and three-point finite-difference schemes. The computer program was also developed for a comparative study of gear temperatures based on heat-transfer coefficients used in the steady-state program with those based on Eq. (7). Preliminary results were given in the form of snap shots of gear temperature contours at the initial stages of tooth engagement. Because the program does many iterations, it requires considerable time to reach the steady-state equilibrium. Because all the experimental data are at steady-state conditions, it was necessary to run the program for some time to match the experimental data.

The case investigated here is that of a pair of eight-pitch standard spur gears with 28 teeth each running at 10 000 rpm with a normal load per unit face width of 5912 N/cm (3378 lb/in.). The actual jet impingement depth is assumed at 87.5 percent of the tooth height. The resulting temperature history is displayed in three forms. First, at predefined time instants, a scan is made over all elements for the maximum and minimum temperature rise. Then the range is divided into a user-defined number of equal-temperature increments. Each division is thus associated with a temperature level. These levels can be presented in the form of contour plots such as those shown in Fig. 5. The analysis is first carried out neglecting boundary-layer interaction (assuming that the fluid film continues to absorb heat.) The jet is assumed to impinge 5° past the last point of tooth engagement. The temperature range at each instant is divided into 10 equal divisions, or contour levels. Because the gear temperature will continuously vary with time, each contour level will define a different temperature level each time. For example, the first contour level defines a temperature rise of 26.4 °C (47.5 °F) at 0.0167 msec (1°), 35.1 °C (63.1 °F) at 0.05 msec (3°), and 8.5 °C (15.2 °F) at 0.167 msec (10°) after the beginning of tooth engagement.

In order to better visualize the chronological development of the heat wave, contour levels are initially preassigned, and the progress of each contour is monitored step by step. Thus the same temperature history may be displayed in form of the fixed contour levels shown in Fig. 6. The range of the temperature rise during the first cycle of tooth engagement, having been determined as approximately 75 °C (135 °F), is divided into 10 equal divisions starting with the first contour level at 75 °C (135 °F) and ending with 0 °C (0 °F) for the last contour level. The progress of heat-wave propagation can easily be traced through the sequence of the snap shots as the gear tooth moves through engagement given in Fig. 6. First, lower level contours emerge then proceed through the gear tooth, followed by the appearance of higher level contours then a gradual withdrawal of these contours occurs as the contact nears the pitch point. The contours then reemerge as the tooth mesh proceeds through the angle of recess until all the 10 contours are realized at the end of contact. A significant drop in temperature then follows due to the absence of frictional heat and the continued dissipation of heat through the fluid film.

The results may be summarized in a single temperature rise versus time graph (shown in Fig. 7) illustrating how the maximum, average midplane, and average face temperatures on the loaded and coast sides of the tooth vary with time. As indicated in the figure, most of the thermal activity is limited to the duration of tooth engagement. Furthermore the highest temperature is highly localized at the tip of the driving gear and at a point between the lowest point of contact and the pitch point. In the beginning of tooth engagement the tip is significantly hotter than the other localized hot spot.

The influence of boundary-layer interaction, as illustrated in Figs. 8 to 10, accentuates that difference. This can be expected, because at the lower hot spot the fluid film continues to convect heat as the thermal boundary layer has not fully developed as it will when engagement approaches the tip. Thus, while the lower hot spot goes through a temperature rise of 40.75 °C (73.35 °F) during initial engagement, the tip can rise by as much as 96.02 °C (172.84 °F) (Figs. 8 and 9) versus 77.24 °C (139.02 °F) (Figs. 5 and 6) if boundary layer interaction is neglected. Note that the lower hot spot is unaffected by boundary-layer interaction (compare Figs. 5(a) and 8(a)).

When the simulation process is continued to steady state, significant differences in predicted tooth temperatures can arise when boundary-layer interaction is not neglected. This is clearly illustrated in Figs. 11 to 16. The maximum temperature rise predicted with boundary-layer interaction is 119 °C (215 °F) (Figs. 14 and 15) in close agreement with experimental findings shown in Fig. 12 from Townsend (1981), compared with 78 °C (141 °F) (Figs. 11 and 13) without boundary-layer interaction. The errors are more significant when average tooth temperatures are compared. With boundary-layer interaction the average steady-state temperature rises 49 °C (88 °F) (Fig. 15). Without boundary-layer interaction a predicted average steady-state temperature rise of only 14 °C (25 °F) is achieved (Fig. 13).

In Fig. 16 the maximum temperature rise is plotted versus time over the entire simulation period. It is interesting to note that with boundary-layer effects the temperature attains a maximum before steady state is reached and scoring could take place even though the indicated steady-state temperature is below the scoring threshold of the tooth pair.

SUMMARY OF RESULTS

The interaction between the thermal and lubricant boundary layers has been incorporated into a transient thermal analysis program for predicting surface temperatures in high-performance spur gears. As a result of this interaction a portion of the fluid film adjacent to the tooth becomes saturated with heat. This portion continues to spread with time until it covers the entire wetted area. Predicted temperature rise for a given set of gears was found to correlate well with previously measured data. If boundary layer interaction is ignored, the predicted temperature rise at the hottest spot could be off by as much as 42.5 percent. Two hot spots exist on the tooth surface of the driving gear: at the tip of the loaded side and below the pitch point. The gear reaches its hottest temperature before steady-state conditions are achieved. Through the use of prescribed temperature contours, the process of heat-wave propagation through the gear tooth can be animated.

REFERENCES

Anderson, N.E., and Loewenthal, S.H., 1981, "Comparison of Spur Gear Efficiency Prediction Methods," NASA Conference Publication 2210, AVRADCOM Technical Report 82-C-16, pp. 365-382.

Benedict, G.H., and Kelley, B.W., 1961, "Instantaneous Coefficients of Gear Tooth Friction," ASLE Transactions, Vol. 4, pp. 59-70.

Buckingham, E., 1949, Analytical Mechanics of Gears, McGraw-Hill Book Co.

DeWinter, A., and Blok, H., 1974, "Fling-off Cooling of Gear Teeth," Journal of Engineering for Industry, Vol. 96, pp. 60-70.

El-Bayoumy, L.E., Akin, L.S., and Townsend, D.P., 1984, "Parameter Studies of Gear Cooling Using an Automatic Finite Element Mesh Generator," ASME Paper No. 84-DET-155.

El-Bayoumy, L.E., Akin, L.S., and Townsend, D.P., 1985, "An Investigation of the Transient Thermal Analysis of Spur Gears," Journal of Mechanisms, Transmissions, and Automation in Design, Vol. 107, pp. 541-548.

Jefferis, J.A., and Johnson, K.L., 1967-68, "Sliding Friction Between Lubricated Rollers," Inst. Mech. Engrs., Proc. Vol. 182, No. 14, pp. 281-291.

O'Donoghue, J.P., and Cameron, A., 1966, "Friction and Temperature in Rolling Sliding Contacts," ASLE Trans., Vol. 9, pp. 186-194.

Patir, N., and Cheng, H.S., 1977, "Prediction of Bulk Temperature in Spur Gears Based on Finite Element Temperature Analysis," ASLE preprint No. 77-LC-3B-2.

Townsend, D.P., and Akin, L.S., 1981, "Analytical and Experimental Spur Gear Tooth Temperature as Affected by Operating Variables, Journal of Mechanical Design, Vol. 103, pp. 219-226.

Van Heijningen, G.J.J., and Blok, H., 1974, "Continuous as Against Intermittent Fling-Off Cooling of Gear Teeth," Journal of Lubrication Technology, Vol. 96, pp. 529-538.

Zienkiewicz, O.C., 1977, "The Time Dimension Finite Element Approximation to Initial Value - Transient Problems," The Finite Element Method, McGraw-Hill, pp. 569-604.

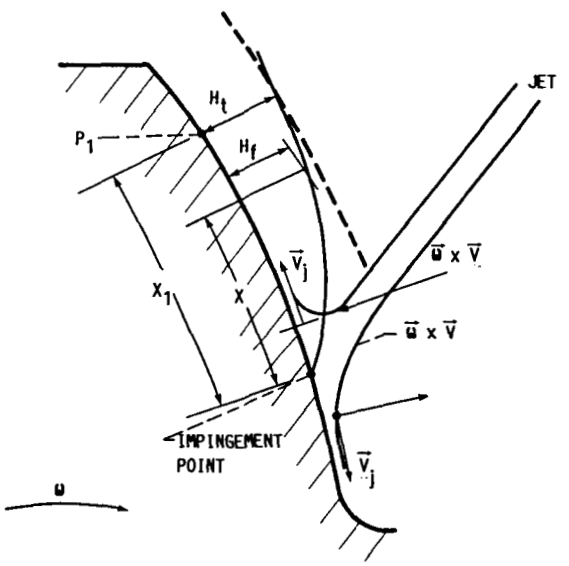

FIGURE 1. - CORIOLIS ACCELERATION ABOVE AND BELOW IMPINGEMENT ON GEAR TOOTH.

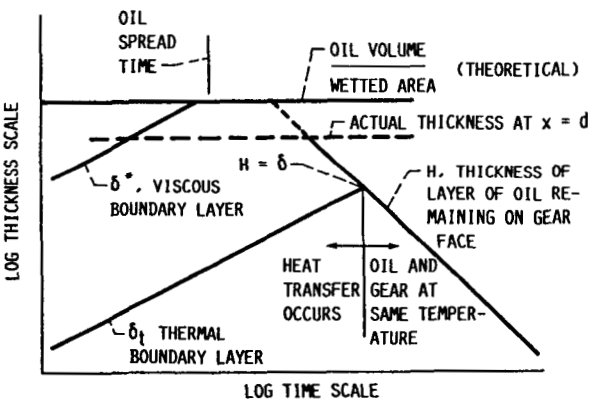

FIGURE 2. - CHARACTERISTIC LENGTH AND TIME SCALES FOR OIL FILM ON ROTATING GEAR TOOTH.

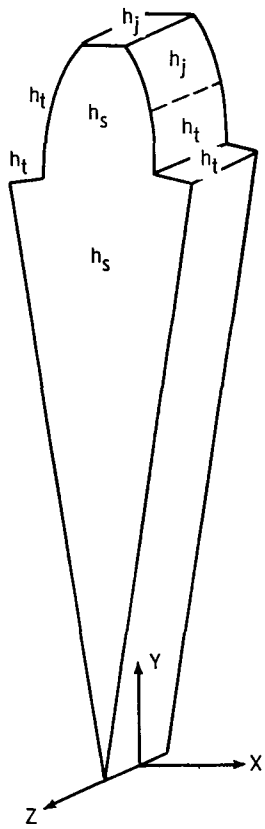

FIGURE 3. - CONVECTIVE HEAT TRANSFER COEFFICIENT ZONES.

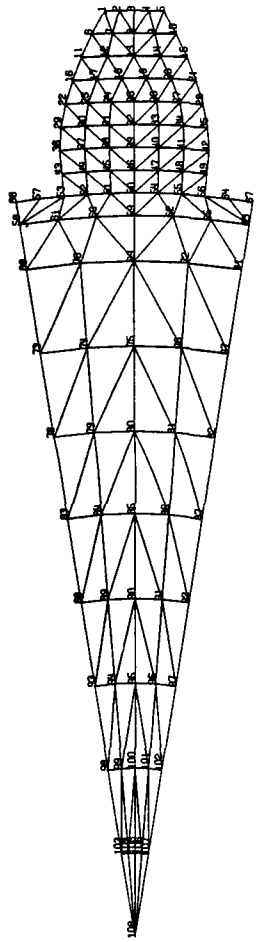

FIGURE 4. - FINITE ELEMENT GRID.

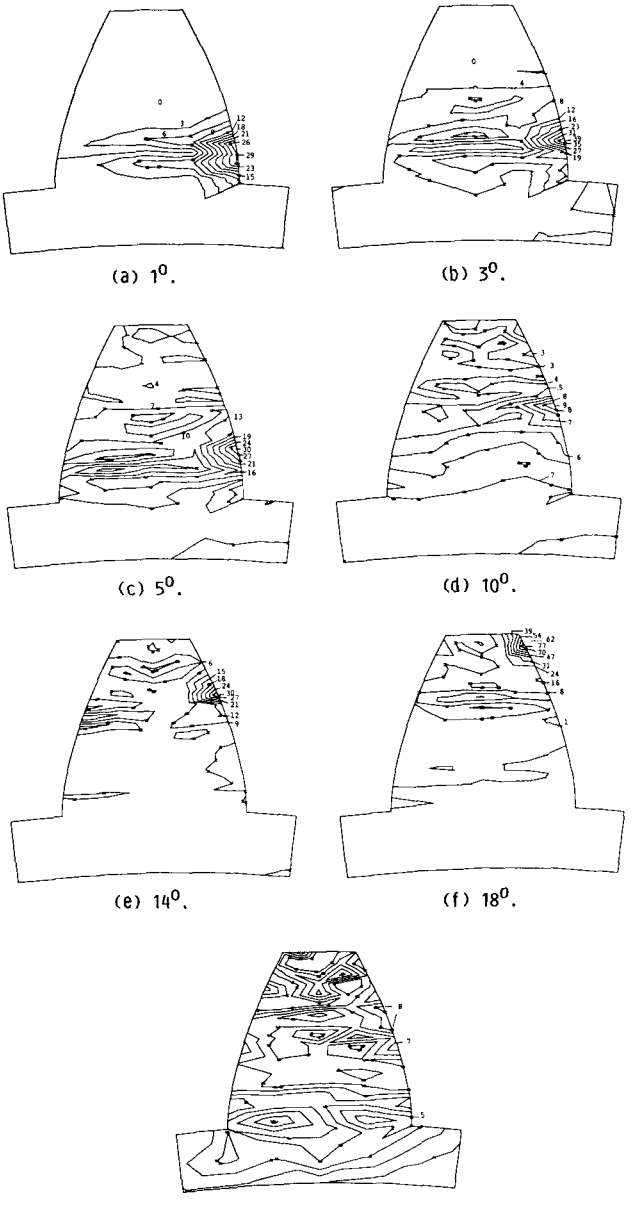

(a) 1^{0}.

(b) 3^{0}.

(c) 5^{0}.

(d) 10^{0}.

(e) 14^{0}.

(f) 18^{0}.

(g) 46.5^{0}.

FIGURE 5. - TEMPERATURE RISE CONTOURS (IN DEGREES CELSIUS) AT 1^{0} TO 46.5^{0} OF GEAR ROTATION AFTER INITIAL TOOTH CONTACT. INITIAL NONEQUILIBRIUM CONDITIONS WITH 10 EQUAL CONTOUR LEVELS BETWEEN MINIMUM AND MAXIMUM TEMPERATURE. SPEED 10 000 RPM; LOAD 5912 N/CM (3378 LB/IN.); 87.5 PERCENT OIL JET IMPINGEMENT DEPTH; NO BOUNDARY LAYER EFFECT.

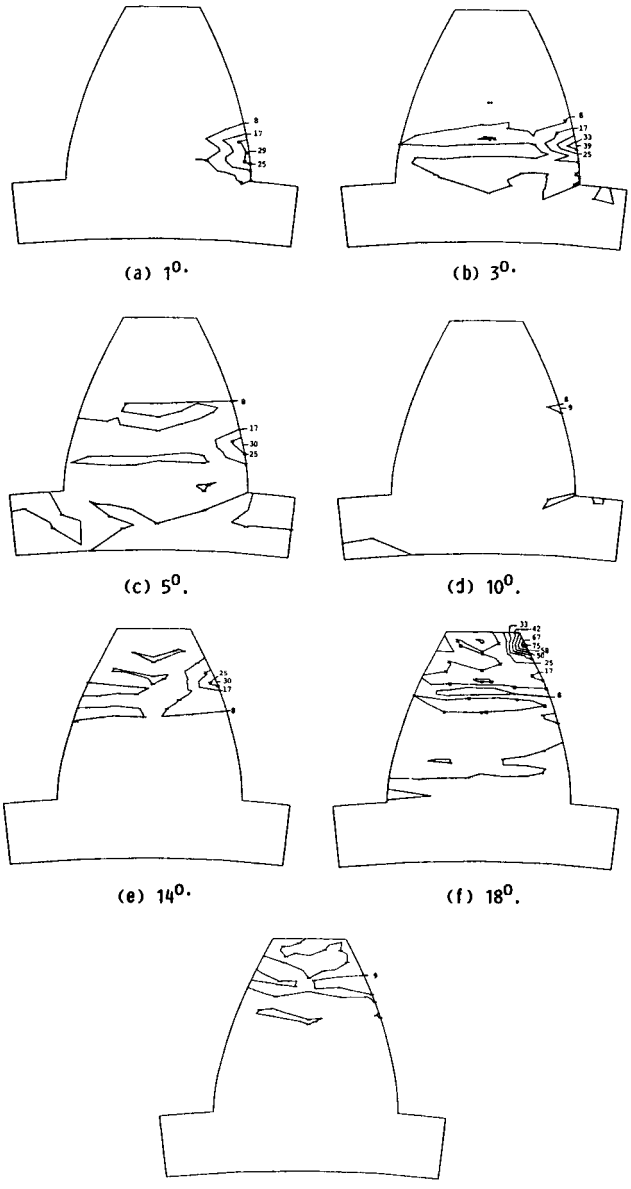

FIGURE 6. - TEMPERATURE RISE CONTOURS (IN DEGREES CELSIUS) AT 1° TO 46.5° OF GEAR ROTATION AFTER INITIAL TOOTH CONTACT. INITIAL NONEQUILIBRIUM CONDITIONS WITH 10 EQUAL PREASSIGNED FIXED CONTOUR LEVELS BETWEEN MINIMUM AND MAXIMUM TEMPERATURE. SPEED 10 000 RPM; LOAD 5912 N/CM (3378 LB/IN.); 87.5 PERCENT OIL JET IMPINGEMENT DEPTH; NO BOUNDARY LAYER EFFECT.

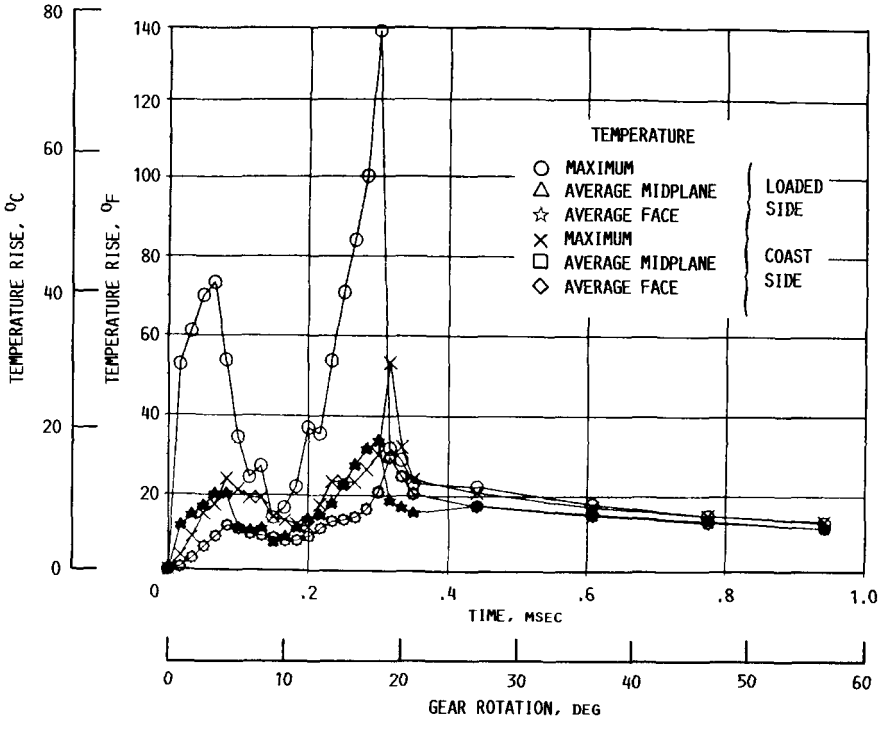

FIGURE 7. - TEMPERATURE RISE VERSUS TIME OR DEGREES ROTATION. INITIAL NONEQUILIBRIUM CONDITIONS. SPEED, 10 000 RPM; LOAD, 5912 N/CM (3378 LB/IN.); 87.5 PERCENT OIL JET IMPINGEMENT DEPTH; NO BOUNDARY LAYER EFFECTS.

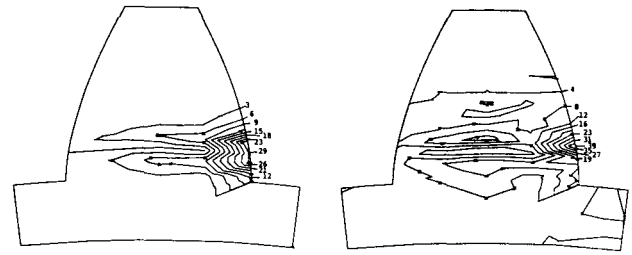

(a) 1^0.

(b) 3^0.

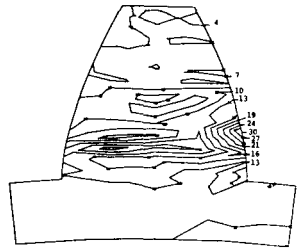

(c) 5^0.

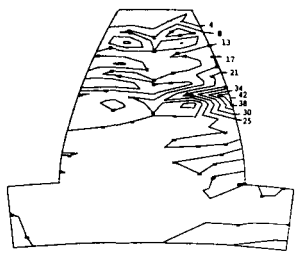

(d) 10^0.

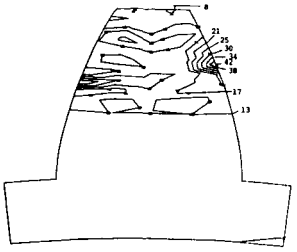

(e) 14^0.

(f) 18^0.

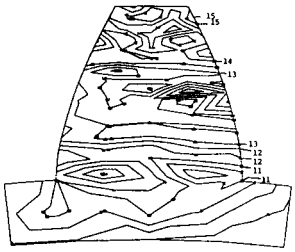

(g) 46.5^0.

FIGURE 8. - TEMPERATURE RISE CONTOURS (IN DEGREES CELSIUS) AT 1^0 TO 46.5^0 OF GEAR ROTATION AFTER INITIAL TOOTH CONTACT. INITIAL NONEQUILIBRIUM CONDITIONS WITH 10 EQUAL CONTOUR LEVELS BETWEEN MINIMUM AND MAXIMUM TEMPERATURE. SPEED, 10 000 RPM; LOAD 5912 N/CM (3378 LB/IN.); 87.5 PERCENT OIL JET IMPINGEMENT DEPTH; WITH BOUNDARY LAYER EFFECT.

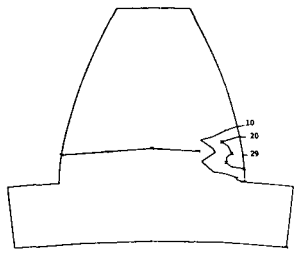

(a) 1^0.

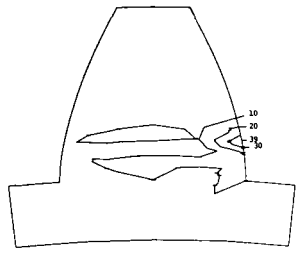

(b) 3^0.

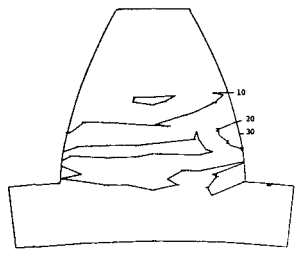

(c) 5^0.

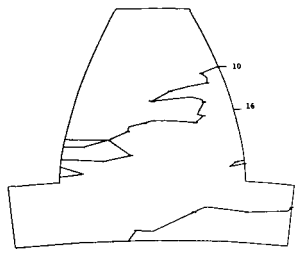

(d) 10^0.

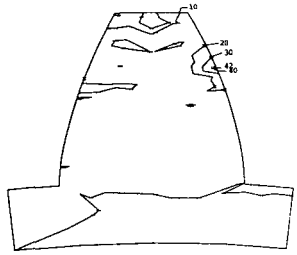

(e) 14^0.

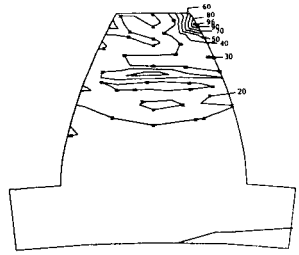

(f) 18^0.

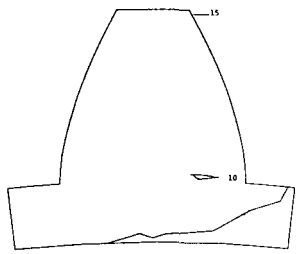

(g) 46.5^0.

FIGURE 9. - TEMPERATURE RISE CONTOURS (IN DEGREES CELSIUS) AT 1^0 TO 46.5^0 OF GEAR ROTATION AFTER INITIAL TOOTH CONTACT. INITIAL NONEQUILIBRIUM CONDITIONS WITH 10 EQUAL PREASSIGNED FIXED CONTOUR LEVELS BETWEEN MINIMUM AND MAXIMUM TEMPERATURE. SPEED, 10 000 RPM; LOAD, 5912 N/CM (3378 LB/IN.); 87.5 PERCENT; OIL JET IMPINGEMENT DEPTH; WITH BOUNDARY LAYER EFFECTS.

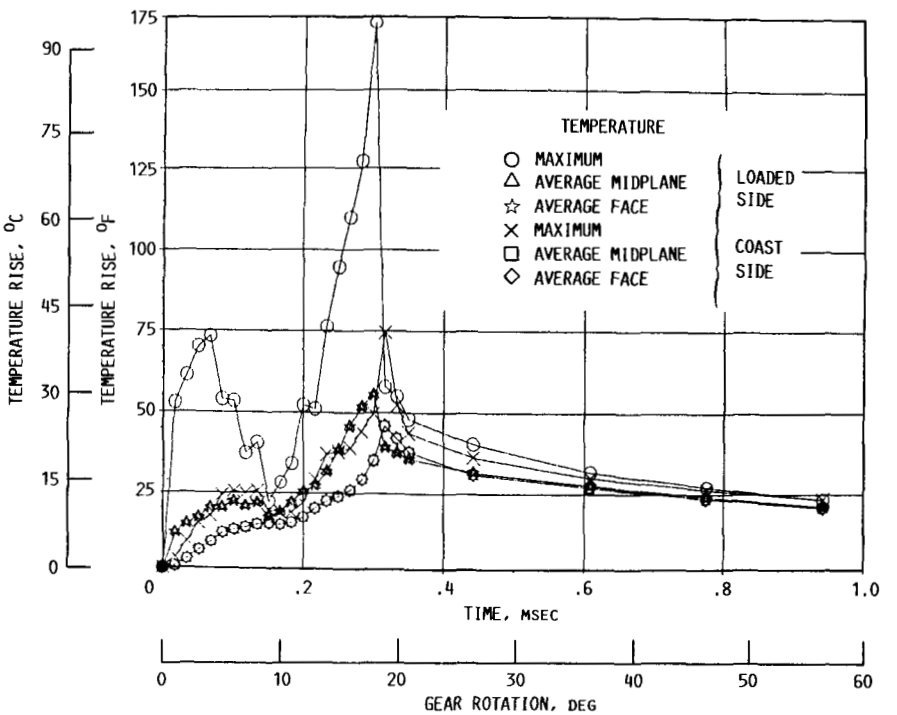

FIGURE 10. - TEMPERATURE RISE VERSUS TIME AND ROTATION. INITIAL NONEQUILIBRIUM CONDITIONS. SPEED, 10 000 RPM; LOAD, 5912 N/CM (3378 LB/IN.); 87.5 PERCENT OIL JET IMPINGEMENT DEPTH; WITH BOUNDARY LAYER EFFECTS.

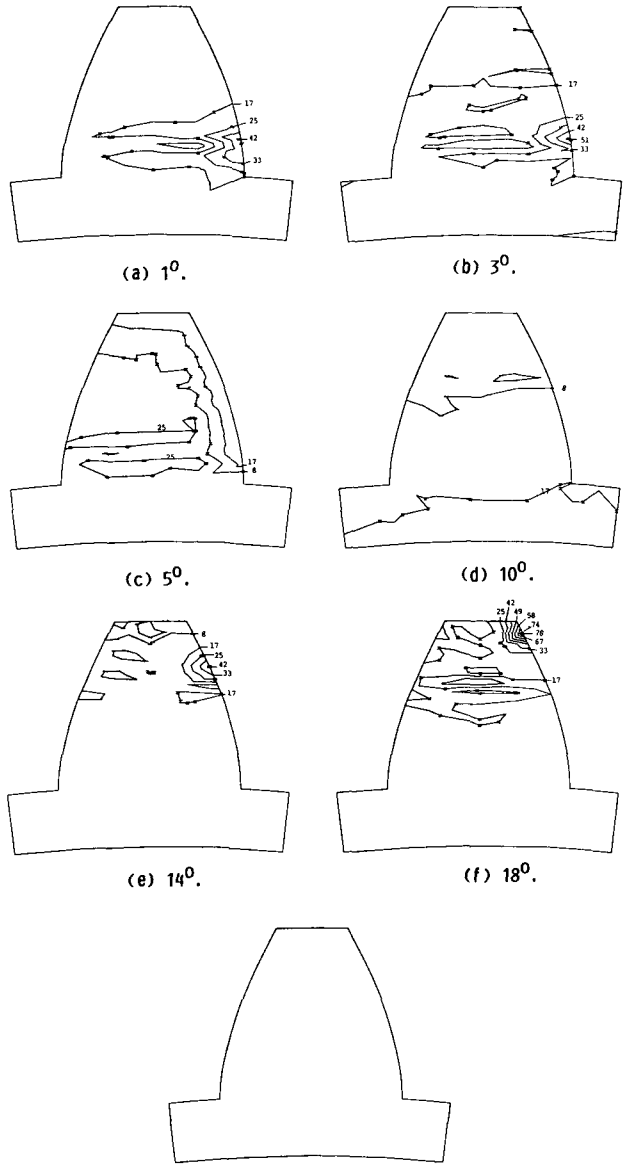

FIGURE 11. - TEMPERATURE RISE CONTOURS (IN DEGREES CELSIUS) AT 1° TO 46.5° OF GEAR ROTATION AFTER INITIAL TOOTH CONTACT. WITH 10 EQUAL PREASSIGNED FIXED CONTOUR LEVELS BETWEEN MINIMUM AND MAXIMUM TEMPERATURE. SPEED, 10 000 RPM; LOAD, 5912 N/CM (3378 LB/IN.); 87.5 PERCENT OIL JET IMPINGEMENT DEPTH; WITHOUT BOUNDARY LAYER EFFECTS AFTER STEADY-STATE EQUILIBRIUM CONDITIONS.

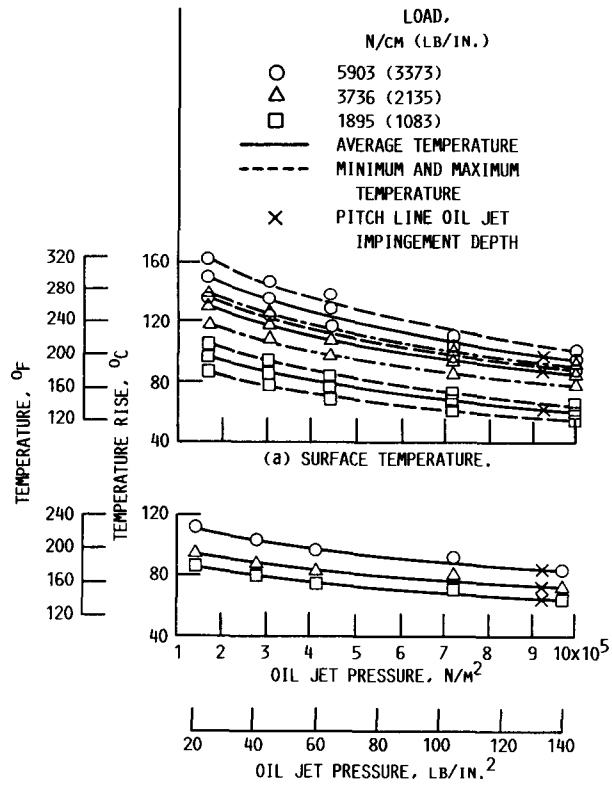

FIGURE 12. - I.R. MICROSCOPE AND THERMOCOUPLE MEASUREMENT OF GEAR TEMPERATURE VERSUS OIL JET PRESSURE FOR THREE LOADS, SPEED, 10 000 RPM; OIL JET DIAMETER, 0.08 CM (0.032 IN.); INLET OIL TEMPERATURE, 308 K (95 °F).

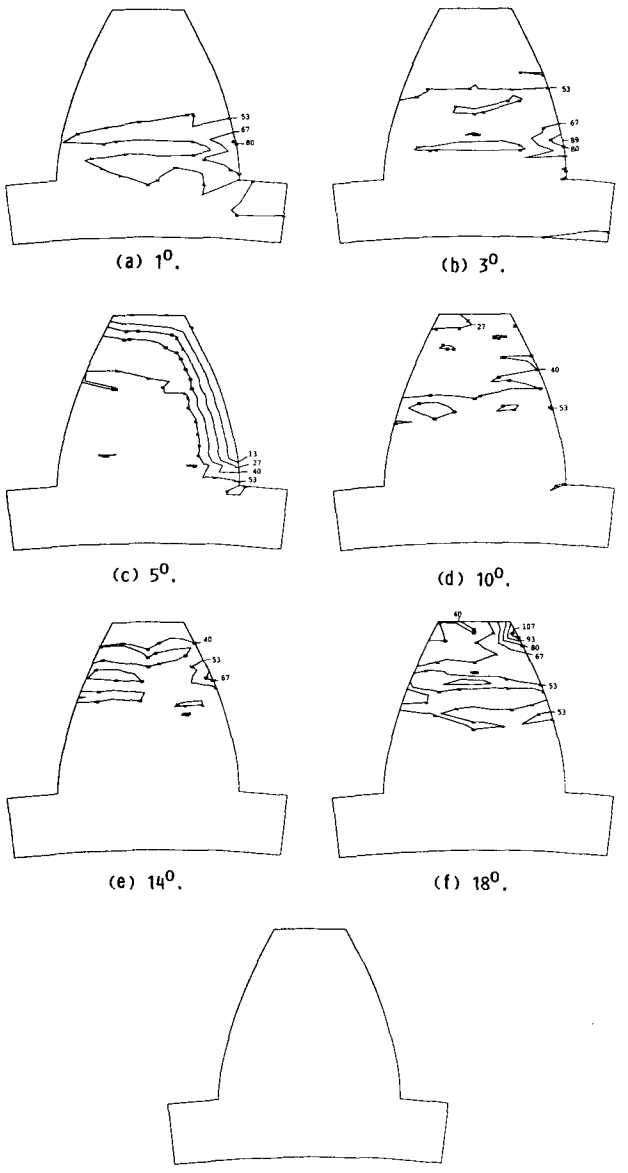

FIGURE 14. - TEMPERATURE RISE CONTOURS (IN DEGREES CELSIUS) AT 1^{0} TO 46.5^{0} OF GEAR ROTATION AFTER INITIAL CONTACT AFTER 63 GEAR REVOLUTIONS. WITH 10 EQUAL PREASSIGNED FIXED CONTOUR LEVELS BETWEEN MINIMUM AND MAXIMUM TEMPERATURE. SPEED, 10 000 RPM; LOAD 5912 N/CM (3378 LB/IN.); 87.5 PERCENT OIL JET IMPINGEMENT; WITH BOUNDARY LAYER EFFECTS.

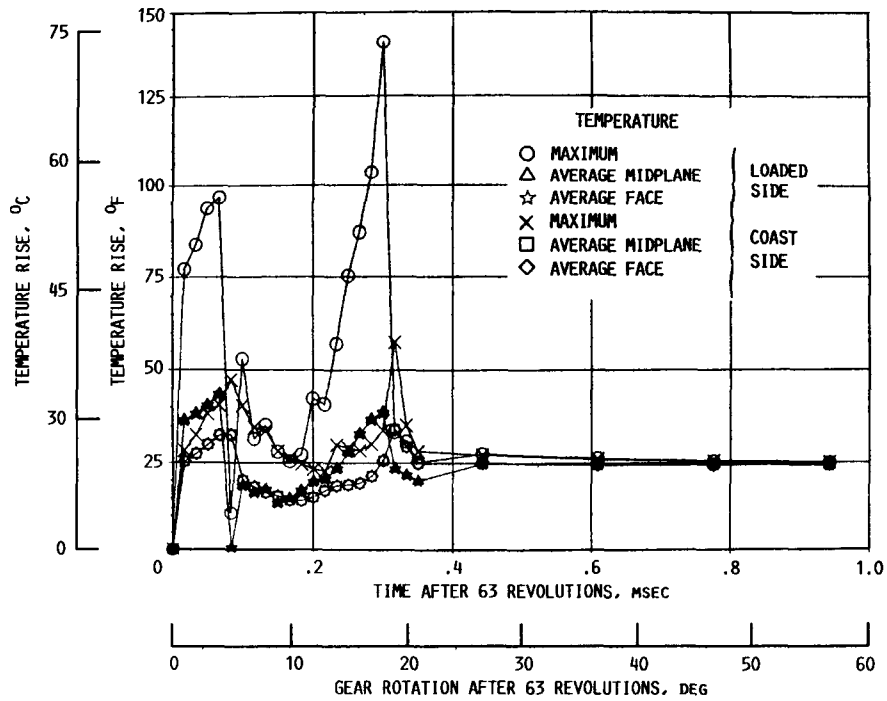

FIGURE 13. - TEMPERATURE RISE VERSUS TIME OR GEAR ROTATION AFTER 63 REVOLUTIONS. SPEED, 10 000 RPM; LOAD, 5912 N/CM (3378 LB/IN.); 87.5 PERCENT OIL JET IMPINGEMENT DEPTH; WITHOUT BOUNDARY LAYER EFFECTS AFTER STEADY-STATE EQUILIBRIUM CONDITIONS.

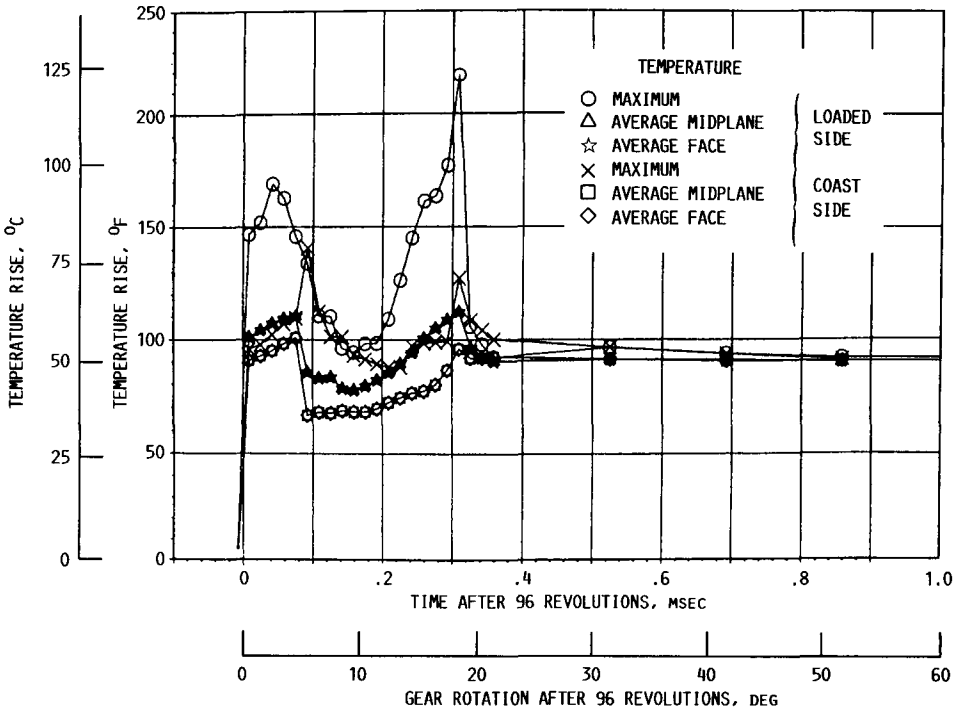

FIGURE 15. - TEMPERATURE RISE VERSUS TIME OR DEGREES ROTATION AFTER 96 REVOLUTIONS. SPEED, 10 000 RPM; LOAD, 5912 N/CM (3378 LB/IN.); 87.5 PERCENT OIL IMPINGEMENT DEPTH AND WITH BOUNDARY LAYER EFFECTS AFTER STEADY-STATE EQUILIBRIUM.

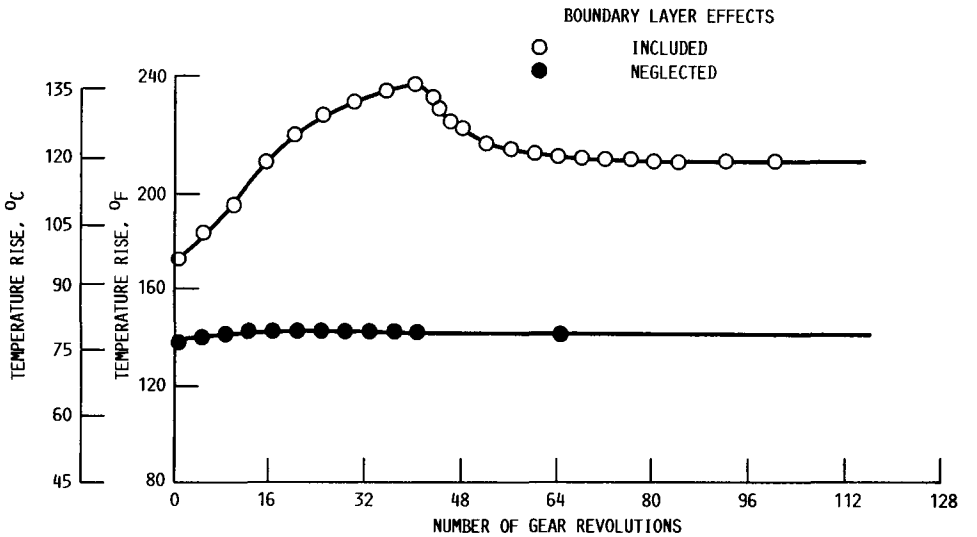

FIGURE 16. - PROFILE MAXIMUM TEMPERATURE VERSUS GEAR REVOLUTIONS WITH AND WITHOUT BOUNDARY LAYER EFFECTS.

NASA
National Aeronautics and Space Administration

Report Documentation Page

1. Report No.	2. Government Accession No.	3. Recipient's Catalog No.
NASA TM-101435 AVSCOM TR-88-C-032		

4. Title and Subtitle

The Role of Thermal and Lubricant Boundary Layers in the Transient Thermal Analysis of Spur Gears

5. Report Date

6. Performing Organization Code

7. Author(s)

L.E. El-Bayoumy, L.S. Akin, D.P. Townsend, and F.C. Choy

8. Performing Organization Report No.

E-4413

9. Performing Organization Name and Address

NASA Lewis Research Center
Cleveland, Ohio 44135-3191
and
Propulsion Directorate
U.S. Army Aviation Research and Technology Activity—AVSCOM
Cleveland, Ohio 44135-3127

10. Work Unit No.

1L162209A47A
505-63-51

11. Contract or Grant No.

12. Sponsoring Agency Name and Address

National Aeronautics and Space Administration
Washington, D.C. 20546-0001
and
U.S. Army Aviation Systems Command
St. Louis, Mo. 63120-1798

13. Type of Report and Period Covered

Technical Memorandum

14. Sponsoring Agency Code

15. Supplementary Notes

Prepared for the Fifth International Power Transmission and Gearing Conference sponsored by the American Society of Mechanical Engineers, Chicago, Illinois, April 25-27, 1989. L.E. El-Bayoumy and L.S. Akin, California State University, Long Beach, California 90840; D.P. Townsend, NASA Lewis Research Center; F.C. Choy, University of Akron, Akron, Ohio 44325.

16. Abstract

An improved convection heat-transfer model has been developed for the prediction of the transient tooth surface temperature of spur gears. The dissipative quality of the lubricating fluid is shown to be limited to the capacity extent of the thermal boundary layer. This phenomenon can be of significance in the determination of the thermal limit of gears accelerating to the point where gear scoring occurs. Steady-state temperature prediction is improved considerably through the use of a variable integration time step that substantially reduces computer time. Computer-generated plots of temperature contours enable the user to animate the propagation of the thermal wave as the gears come into and out of contact, thus contributing to better understanding of this complex problem. This model has a much better capability at predicting gear-tooth temperatures than previous models.

17. Key Words (Suggested by Author(s))	18. Distribution Statement
Lubrication; Heat transfer; Gears; Cooling; Friction heating; Thermal boundary layer	Unclassified – Unlimited Subject Category 37

19. Security Classif. (of this report)	20. Security Classif. (of this page)	21. No of pages	22. Price*
Unclassified	Unclassified	16	A03

NASA FORM 1626 OCT 86

*For sale by the National Technical Information Service, Springfield, Virginia 22161